Plasma-Etching Induced Damage in Thin Oxide

Hyungcheol Shin and Chenming Hu

University of California at Berkeley
Department of Electrical Engineering and Computer Sciences
and the Electronics Research Laboratory
Berkeley, California 94720
TEL: (510) 642-1010, FAX: (510) 642-2916

Abstract

Plasma Al etching and resist ashing processes cause Fowler-Nordheim current to flow through the oxide and plasma-induced damage can be simulated and modeled as damage produced by constant current electrical stress. These current produced by plasma process increases with the "antenna" size of the device structure. CV measurement is a more sensitive technique for characterizing plasma-etching induced damage than oxide breakdown. The stress current is collected only through the aluminum surfaces not covered by the photoresist during plasma processes. The plasma stress current is proportional to Al pad peripheral length during Al etching and Al pad area during photoresist stripping. A model of oxide damage due to plasma etching is proposed.

Introduction

Plasma processes have been widely used in VLSI manufacturing for Aluminum etching and photoresist stripping. In the plasma ambient, reactive ions generated in the discharge are accelerated by the self bias voltage and collide with the surface of the wafer. These ions can cause damage to the wafer. Degradation of gate oxides in MOS devices due to the plasma process has been observed and attributed to electrostatic charging during the process [1]-[9]. In the plasma ambient, charges are collected by aluminum pads, which serve as "antennas". The stress can cause trapped charges in the oxide as well as surface states at SiO_2-Si interface, therefore decrease the breakdown voltage and deform the CV curve of the gate oxide. In this study, we use breakdown voltage and CV to determine the amount of stress during the process.

Experiment

The test structures used are polysilicon-gate MOS capacitors fabricated on n-type (100) silicon substrate with 6.4 nm and 11.6 nm gate oxide grown in dry oxygen at 900 °C. After gate definition, 500 nm aluminum was deposited. Aluminum etching was done in Lam Research Autoetch 690B system and the photoresist ashing was done in a Technics Micro-stripper Series 200 plasma system for one hour. To characterize the damage during the plasma processes, the oxide integrity was monitored after each step. Changes in the ramp breakdown voltages or quasi-static CV curves after each step are used to determine the stress current produced by each plasma step. Control wafers receiving only wet-etching were also fabricated. If the plasma-induced damage is due to electrostatic charging, the damage to gate oxide should be identical to that produced by applying a constant current to the gate electrode for a duration equal to the process time. The current would correspond to that collected by the antennas.

Results and Discussions

Fig. 1 shows the ramp breakdown voltage distribution of large capacitors (1 mm^2) with 9 mm^2 metal pads after Al plasma etching and photoresist ashing steps. Oxides with initial breakdown voltage less than 10 V became shorts after Al etching (B). About 70% of the devices are broken down after photoresist stripping (C).

The breakdown statistics of intrinsic(very small area) capacitors were measured to investigate the effect of different metal areas to oxide area ratios(antenna effect) and the spatial uniformity of the process induced stress current. Fig. 2 shows that there is very little change in the intrinsic breakdown strength for oxides subjected to Al plasma etching only(B). However, plasma ashing causes significant reduction in breakdown strength even for intrinsic oxides. Capacitors with larger metal pads have higher failure rates as expected. However, the plasma-induced stress current(or voltage) varies for a given metal to oxide area ratio as extracted from the large variation in breakdown voltage for small area capacitors after processing shown in Fig. 2. This non-uniformity is fairly random(as oppose to radially distributed, for example), as shown in Fig. 3.

Changes in the breakdown voltage can be clearly measured only when the process-induced problem is very severe and using large-area oxide samples(thus making it difficult to study large antenna-to-oxide ratios) and large number of test devices. Even then it cannot give high resolution in quantitative study. Accurate estimation of the amount of charge collection can be obtained by comparing the CV curves of MOS capacitors after plasma process with control devices after electrical stress. Fig. 4 shows the effect of the electrical stressing on CV curve. Fig. 5 shows the quasi-static CV characteristics of capacitors after various processing steps. The difference between the control wafer and the one after aluminum etching is very small, while the CV curve changes dramatically after photoresist ashing. Also note that the plasma-induced damage during Al etch step is not uniform across the wafer as shown in Fig. 6. More damage is observed near the center of the wafer.

Fig. 7 shows the quasi-static CV curves for MOS capacitors with different aluminum pad sizes after pad capacitances were subtracted. The size of the capacitors is 1,600 μm^2 with identical layout except for the size of aluminum pads ranges from 16,000 to 160,000 μm^2. The CV curve for wet-etched capacitor is also shown as curve A. Because larger aluminum pad collects more charge during the etching, the CV curve of capacitors with larger pads show higher degree of degradation. The differences in breakdown voltage and charge to breakdown between A and E are within the ranges of sample to sample random variations. Clearly, CV degradation is a more sensitive technique suitable for process monitor and for quantitative study of the charging process.

Capacitors on wet-etched control wafers had identical CV (curve A in Fig. 7) independent of the Al geometry. They were stressed by passing different levels of constant current through the gate for the same length as the plasma etching time to generate a series of reference curves, as shown in Fig. 8. Also shown in the figure is the CV curve of a capacitor with 16,000 μm^2 aluminum pad etched in plasma. This curve matches the reference curve of 10 nA stressing very well, indicating that the 16,000 μm^2 Al pad(Curve B in Fig. 7) collected 10 nA(curve C in Fig. 8) of plasma charging current during the etching process. Note from Fig. 8 that this technique can infer a range of plasma charging current covering many orders of magnitude. By using the same method, the plasma charging current for each test capacitor can be extracted with a high resolution.

Fig. 9 shows the extracted stress current due to plasma etching at different locations across the wafer for three different power levels. There is a radial variation of stressing for devices from the wafer center to the edge. The after-stress CV curves of the wet-etched sample showed no position dependence. The radial distribution of the stress current during etching results from the radial distribution of the plasma intensity and etch rate in this etcher.

Fig. 10 shows the plasma stressing current during Al etching as a function of Al pad peripheral lengths for devices located about 2 cm from the wafer center. The stress current for the devices during aluminum etching shows obvious pad-size dependency, i.e., antenna effect. The slope is about 1, independent of the shape of Al pads. Clearly, the stressing current does not increase in proportion to the Al pad area. Rather, it is proportional to the peripheral length of Al pads. The implication is that only the Al surface exposed to the plasma can collect current and contribute the antenna effect.

Fig. 11 shows the stressing current time product during plasma photoresist stripping as a function of square aluminum pad *areas*. For this experiment, Al etching was done by wet process to avoid the plasma damage during Al etching. The slope of all the lines is about 1. Clearly, the plasma stressing current is roughly proportional to the area of the Al pads. We interpret this as saying that most of the damage is done after the photoresist is stripped such that the entire Al pads are exposed. To support this interpretation, capacitors with bare Al pads previously patterned by wet etching were put through the photoresist stripping process even though the photoresist had already been removed by a wet process. The stressing current was also found to be proportional to the pad area(Fig. 12). The measured value of stress current time product is 15 $nA \cdot s/\mu m^2$. This is about four times larger than the value in Fig. 11. This is due to the fact that for the latter case the device collected the charges during all the process whereas, in the former case the stress current is collected only after the Al is exposed. The factor of four is roughly equal to the ratio of the total resist stripping time to the over-stripping time.

During rf plasma processes, the surface of the wafer collects conduction current from the plasma which is composed of steady ion current and pulsed electron current [10]. Therefore, the plasma process can better be modeled as a bi-directional current stress. For simplicity, however, we have arbitrarily modeled the stress current as a DC current. We feel that this simplification can be refined at a later time. The magnitude of the ion current during plasma etching is given by

$$J_i = \varepsilon_0 \left(\frac{2e}{M}\right)^{\frac{1}{2}} \frac{V_0^{\frac{3}{2}}}{s^2} \qquad (1)$$

where ε_0 is permittivity, e is electronic charge, M is ion mass, V_0 is the DC voltage across two plates and s is the sheath thickness. The DC voltage V_0 was measured to be 120 volts at 250 watts and 400 volts at 500 watts. The sheath thickness s is assumed to be 5 mm. Fig. 13 compares the calculated ion current with the stress current deduced from the CV measurement for different power levels. The experimental value and the calculated ion current value is of the same order of magnitude and the difference is attributed to the electron current component and possibly the enhanced rate of interface trap generation under AC stress [11].

Summary

Plasma-induced damage can be simulated and modeled as damage produced by constant current electrical stress. These current produced by plasma process increases with the antenna size of the device structure. Plasma processing is shown to produce severe distortions in the oxide CV characteristics, from which one can easily deduce the equivalent current during processing. A clear radial variation of stressing is found for plasma etching process. The stress current is collected only through the aluminum surfaces not covered by the photoresist during plasma processes. A model of oxide damage due to plasma etching is proposed.

ACKNOWLEDGEMENT

This research is sponsored by SRC, Sandia Laboratory, Signetics, TI, Rockwell International and AMD under MICRO program and ISTO/SDIO administered by ONR under Contract N00014-85-K-0603.

REFERENCES

[1] C. Gabriel and J. C. Mitchener, "Reduced device damage using an ozone based photoresist removal process," *Proc. SPIE*, vol. 1086, pp. 598- 603, 1989.

[2] F. Shone, K. Wu, J. Shaw, E. Hokelet, S. Mittal, and A. Haranahalli, "Gate oxide charging and its elimination for metal antenna capacitor and transistor in VLSI CMOS double layer metal technology," *Sym. VLSI Tech. Dig. papers*, pp. 73-74, 1989.

[3] Y. Kawamoto, "MOS gate insulator breakdown caused by exposure to plasma," *Proc. 1985 Dry Process Symp., The Inst. Elect. Eng. of Japan*, pp. 132-137, Oct. 1985.

[4] K. Tsunokuni, K. Nojiri, S. Kuboshima, and K. Hirobe, "The effect of charge build-up on gate oxide breakdown during dry etching," *Extended Abstracts of the 19th Conf. on Solid State devices and Materials*, pp.195-198, 1987.

[5] I.-W. Wu, R.H. Bruce, G.B. Anderson, M. Koyanagi, and T.Y. Huang, " Damage to gate oxides in reactive ion etching," *Proc. SPIE*, vol. 1185, pp. 284-295, 1989.

[6] S. Fang and J. Mcvittie, "Thin-Oxide Damage from Gate Charging During Plasma Processing," *IEEE Electron Devices Lett.*, vol.13, no 5, pp. 288-290, May. 1992.

[7] H. Shin, C.-C. King, T. Horiuchi and C. Hu, "Thin oxide charging current during plasma etching of aluminum," *IEEE Electron Devices Lett.*, vol.12, no 8, pp. 404-406, Aug. 1991.

[8] H. Shin, C. King and C. Hu, "Thin Oxide Damage by Plasma Etching and Ashing Processes," *Proc. IRPS*, pp.37-41, 1992.

[9] S. Fang and J. Mcvittie, "A Model and Experiments for Thin Oxide Damage from Wafer Charging in Magnetron Plasmas," *IEEE Electron Devices Lett.*, vol.13, no 6, pp. 347-349, Jun. 1992.

[10] D. Graves and M. Surendra, "Modeling and Simulation of Plasma Processes," in *IEDM Tech. Dig.*, p 887, 1991.

[11] E. Rosenbaum, Z. Liu, and C. Hu, "The Effect of Oxide Stress Waveform on MOSFET Performance," in *IEDM Tech. Dig.*, p 719, 1991.

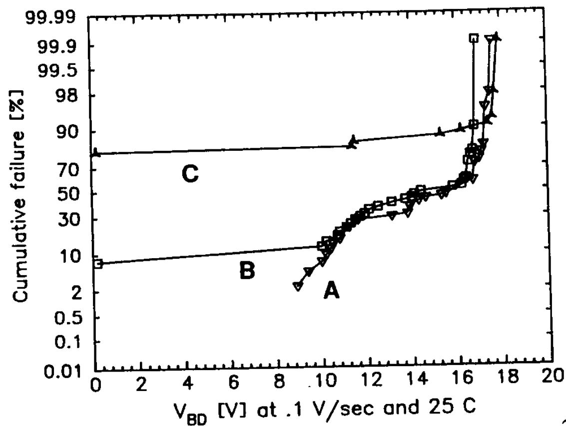

Fig. 1. Breakdown voltage distribution of capacitors with 1 mm^2 active area, 11.6 nm thick oxide after different processes. Oxides with initial breakdown voltage less than 10 V became shorts after Al etching(B). About 70% of the devices are broken down after photoresist stripping(C).

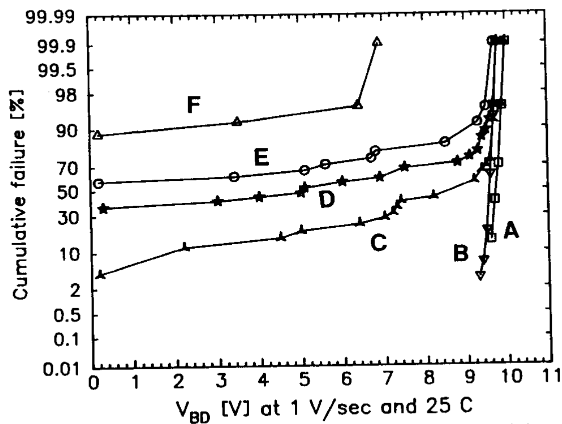

Fig. 2. Cumulative failure vs. breakdown voltage for 6.4 nm capacitors with area = 40 μm x 40 μm under different processing conditions and antenna ratios (R). A: control wafer, B: plasma Al etching, R=300, C: condition B + plasma PR ashing for 1 hour, R=10, D: same as C, R=30, E: same as C, R=50, F: same as C, R=100.

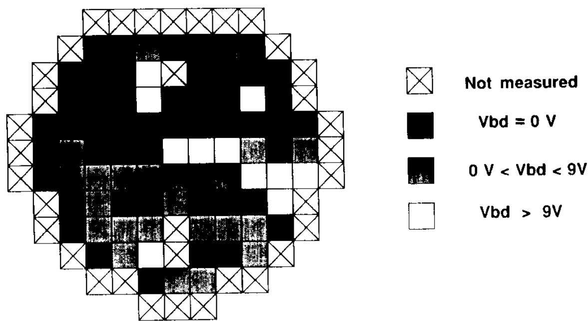

Fig. 3. Distribution of breakdown voltage for 6.4 nm capacitors with area = 40 μm x 40 μm, R=50, over the wafer.

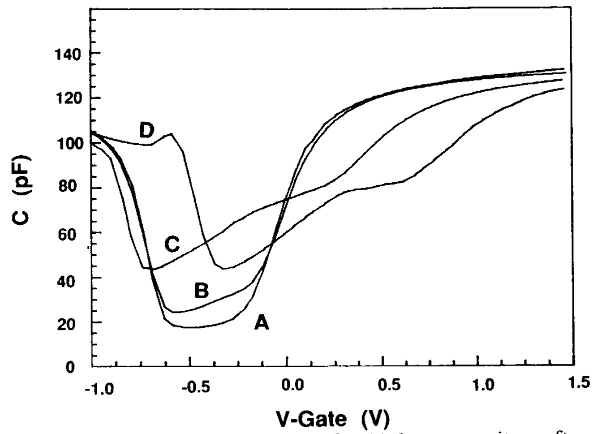

Fig. 4. The quasi-static CV curve for 11.6 nm capacitors after electrical stress for one hour. A:Initial, B: 9V, C:11V, and D:12V.

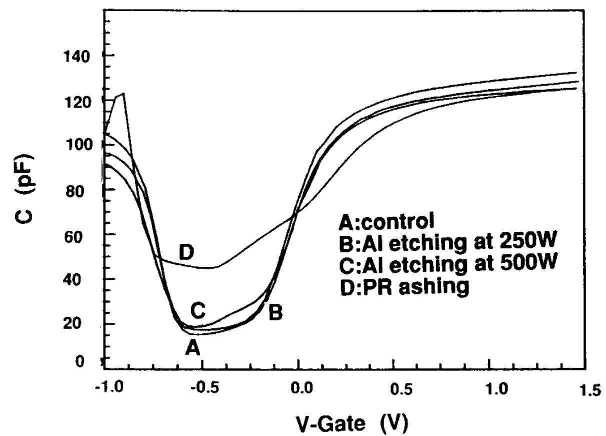

Fig. 5. Quasi-static CV curves of capacitors with 40,000 μm^2 active area, 11.6 nm thick oxide after different processes. A: control wafer (Al wet-etched), B: plasma Al etching for 60 seconds at 250 watts, and D: condition B + plasma PR ashing for one hour.

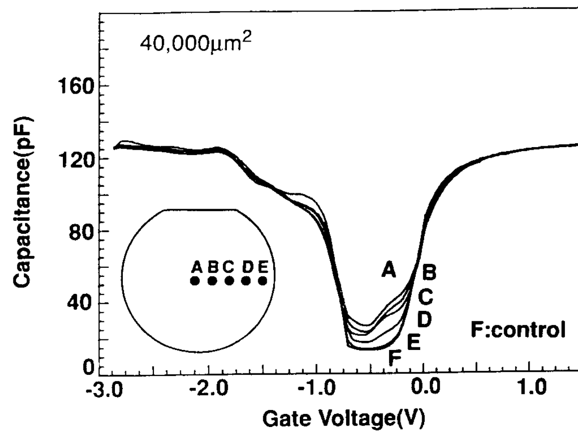

Fig. 6. The quasi-static CV curves for 11.6 nm capacitors after 60 seconds plasma etching of Al at five different positions on a wafer. CV deformation is larger at the wafer center where the plasma density is larger. Curve F is the CV of wet etched samples.

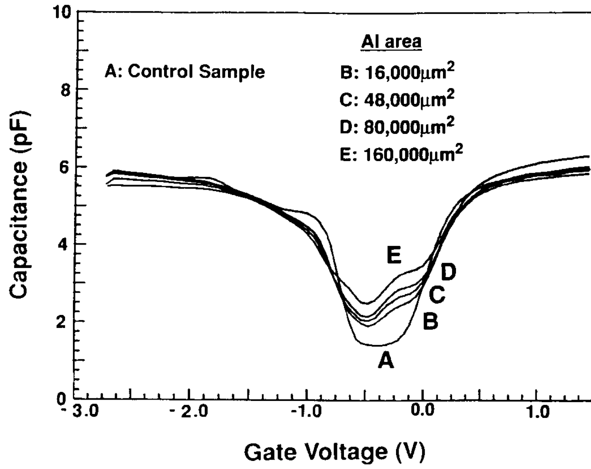

Fig. 7. 1,600 mm2, 11.6 nm oxide CV after 60s plasma etching of Al. curve A is the CV of wet etched samples.

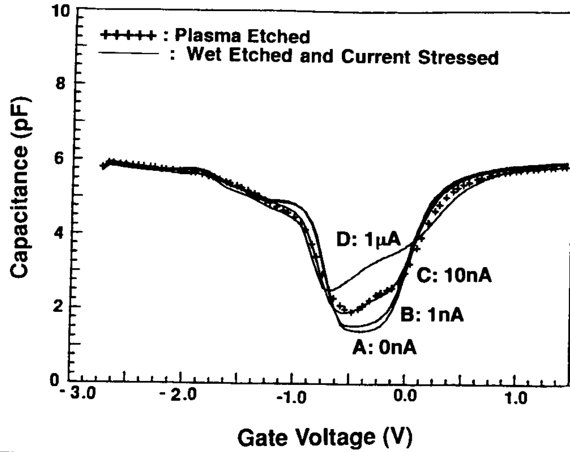

Fig. 8. CV after 60 s plasma etching of Al and after constant current stress for 60 s at varying current level. Curve A is the CV of control samples. The CV after plasma etching matches very well with CV after 10 nA stress.

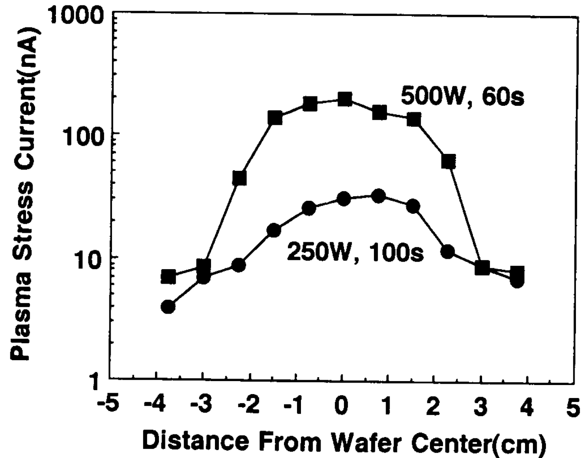

Fig. 9. The extracted plasma stress current shows a clear radial distribution across the wafer.

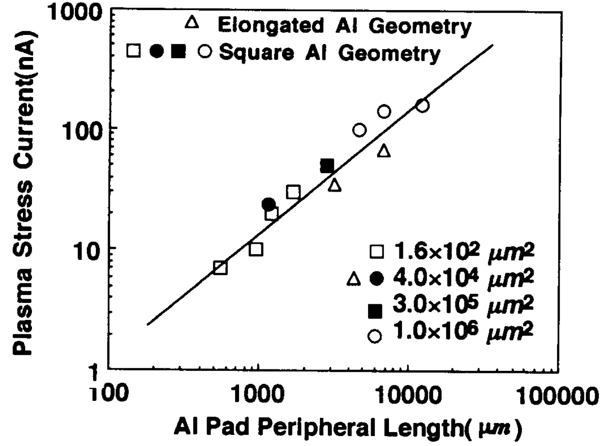

Fig. 10. The plasma stress current during the etching is approximately proportional to the Al edge length, independent of the oxide areas and the Al pads shape.

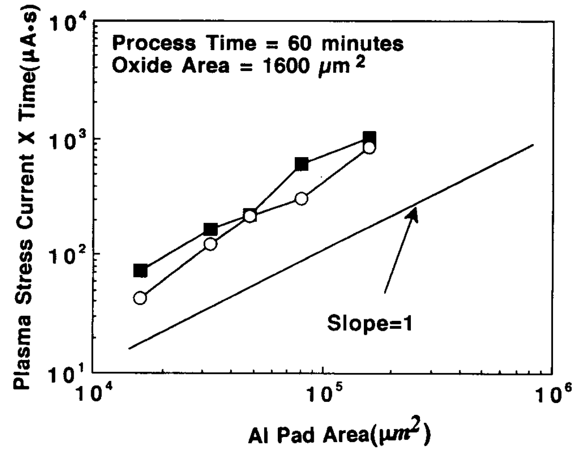

Fig. 11. Since the entire surface of the Al pad can collect charges from plasma, the plasma stress current during plasma photoresist stripping is proportional to electrode area. The two curves are for different locations on the wafer. The process time is 60 minutes.

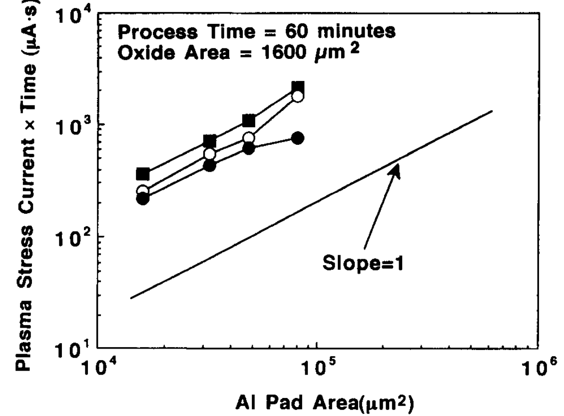

Fig. 12. The plasma stress current under plasma photoresist stripping condition without any resist present is also proportional to the Al pad area. The current is about four times larger than in the previous figure. Three sets of data taken from different positions are shown.

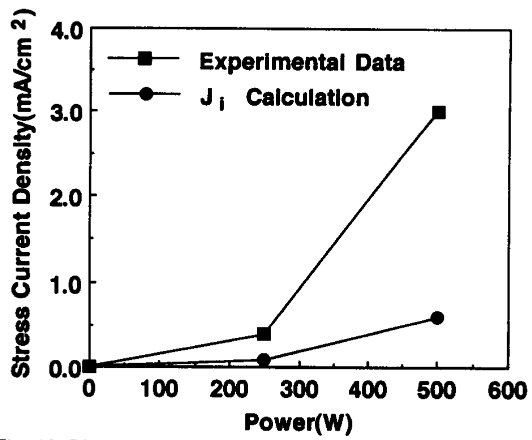

Fig. 13. Plasma stress current per unit area of exposed Al surface and predicted ion current density at different powers.